

A similarity reduction of the generalized Grad-Shafranov equation

A. I. Kuiroukidis¹, D. A. Kaltsas^{1,2} and G. N. Throumoulopoulos¹

¹Department of Physics, University of Ioannina, GR 451 10 Ioannina, Greece

²Department of Physics, International Hellenic University, Kavala, Greece, GR 654 04

Emails: a.kuirouk@uoi.gr, kaltsas.d.a@gmail.com, gthroum@uoi.gr

Abstract

We extend previous work [Y. E. Litvinenko, Phys. Plasmas **17**, 074502 (2010)] on a direct method for finding similarity reductions of partial differential equations such as the Grad-Shafranov equation (GSE), to the case of the generalized Grad-Shafranov equation (GGSE) with arbitrary incompressible flow. Several families of analytic solutions are constructed, the generalized Solovév solution being a particular case, which contain both the classical and non-classical group-invariant solutions to the GGSE. Those solutions can describe a variety of equilibrium configurations pertinent to toroidal magnetically confined plasmas and planetary magnetospheres.

1 Introduction

The analysis of similarity reductions of partial differential equations plays a crucial role in many physical applications. Some time ago in [1] a direct method for finding similarity reductions of the Grad-Shafranov equation (GSE) has been introduced, thus generalizing previous work [2] on the subject. This was then generalized [3] for the case of the generalized Grad-Shafranov equation (GGSE) (equation (1) below), i.e. using classical Lie-group methods to find a one-parameter group admitted by the equation and the corresponding group-invariant solution.

The Solovév solution [4] and the Herneger-Maschke solution [5] are among the most widely employed analytical solutions of the GSE, the former corresponding to toroidal current density non-vanishing on the plasma boundary while the later to toroidal current density vanishing thereon. In the presence of flow, which plays a role in the transition to improved confinement modes in tokamaks, the equilibrium satisfies a GGSE in general coupled with a Bernoulli equation involving the pressure [6, 7]. For incompressible flow, the density becomes a surface quantity and we obtain the GGSE [7, 8]. Generalized Solovév solutions of the GGSE were derived in [8, 9] and asymptotic expansion solutions to the general linearized GGSE in [10, 11].

A symmetry group of a partial differential equation is a set of transformations of the independent or/and dependent variables that allows to generate new classes of solutions from a single solution known. Symmetry properties of a system of Euler-type equations were studied in [12]. Symmetry properties and solutions to the GSE and the GGSE were studied in [13, 14], whereas symmetry methods for differential equations are exposed in [15]. Translationally symmetric force-free states are constructed in [16]. The literature on exact solutions to the GSE is extensive and a brief reference list includes [17, 18], while other symmetry and similarity reduction methods were employed in [19, 20, 21, 22].

Aim of the present study is to construct new families of analytic solutions to the GGSE by using the method of similarity reduction along the lines of [1], describing equilibrium configurations relevant to experimental fusion and space plasmas. The structure of the paper is as follows: In section 2 we present the direct method for finding the similarity reduction of the GGSE and show that the generalized Solovév solution is a particular case of the above mentioned set of solutions. In section 3 we extend the set of solutions to the GGSE and show that all group-invariant solutions of [3] are in fact particular cases of the extended set of solutions. In section 4 we present a new similarity reduction of the GGSE, not considered in [1], associated with solutions which can describe part of planetary magnetospheres. Finally, in section 5 we present a brief discussion on the novel results of this paper.

2 Axisymmetric equilibria with non-parallel flow from similarity reduction

We consider the GGSE in its completely dimensionless form [7, 8]

$$u_{rr} - \frac{1}{r}u_r + u_{zz} + \frac{1}{2}\frac{d}{du}\left[\frac{X^2}{1-M_p^2}\right] + r^2\frac{dP_s}{du} + \frac{1}{2}r^4\frac{d}{du}\left[\rho\left(\frac{d\Phi}{du}\right)^2\right] = 0. \quad (1)$$

Here, employing cylindrical coordinates (z, r, ϕ) , the function $u(r, z)$ relates to the poloidal magnetic flux function and labels the magnetic surfaces; the flux function $X(u)$ relates to the toroidal magnetic field; $P_s(u)$ is the pressure in the absence of flow; $\rho(u)$ is the density; $M_p(u)$ is the Mach function of the poloidal velocity with respect to the respective Alfvén velocity; and $\Phi(u)$ is the electrostatic potential related to the component of the electric field non parallel to the magnetic field. The flux functions $X(u)$, $M_p(u)$, $P_s(u)$, $\rho(u)$ and $\Phi(u)$ remain arbitrary.

Choosing the free function terms to be constant, i.e., $((1/2)d/du[X^2(1 - M_p^2)] = G$, $dP_s/du = F$, $(1/2)d/du[\rho(d\Phi/du)^2] = E$ with G, F, E constants) we have the following form of the GGSE that will be the focus of this study

$$u_{rr} - \frac{1}{r}u_r + u_{zz} + Er^4 + Fr^2 + G = 0. \quad (2)$$

Equation (2) is satisfied by the generalized Solovév-type solution [8]

$$u_{Sol} = \left[z^2 \left(r^2 - \frac{G}{2} \right) - \frac{(F + E + 2)}{8}(r^2 - 1)^2 - \frac{E}{24}(r^2 - 1)^3 \right]. \quad (3)$$

The respective equilibrium configuration inside the separatrix, up-down symmetric with a pair of X-points, is plotted in Fig. 1.

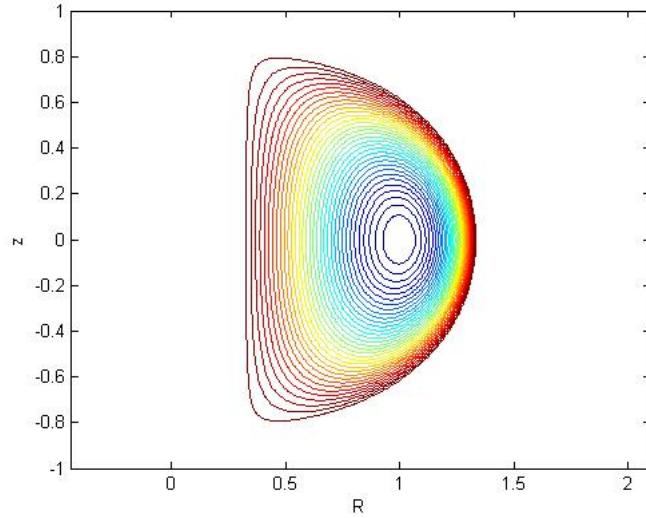


Figure 1: The generalized Solovév equilibrium in connection with the solution (3) of the GGSE for $E = -2$, $G = 0.2$, $F = -4$. The bounding flux surface corresponds to $U_b = 0.34$.

We consider now the similarity reduction of Eq. (2) via the ansatz [1]

$$u(r, z) = \alpha(r, z) + \beta(r, z)w[x(r, z)]. \quad (4)$$

Substituting (4) into (2) we obtain

$$\begin{aligned} \beta(x_r^2 + x_z^2)w'' &+ \left[\left(2\beta_r - \frac{1}{r}\beta \right) x_r + 2\beta_z x_z + \beta(x_{rr} + x_{zz}) \right] w' + \\ &+ \left(\beta_{rr} + \beta_{zz} - \frac{1}{r}\beta_r \right) w + \\ &+ (\alpha_{rr} + \alpha_{zz} - \frac{1}{r}\alpha_r + Er^4 + Fr^2 + G) = 0. \end{aligned} \quad (5)$$

Let us choose as a first illustration of the method the case where $\alpha = \alpha(r)$, $\beta = \beta(r)$ and $x = x(z)$. Then Eq. (5) becomes

$$\beta x_{zz} + (\beta_{rr} - \frac{1}{r}\beta_r)x + (\alpha_{rr} - \frac{1}{r}\alpha_r + Er^4 + Fr^2 + G) = 0. \quad (6)$$

This equation can be satisfied by choosing $x(z) = z^2/2$, provided that the functions α, β satisfy the ordinary differential equations

$$\beta_{rr} - \frac{1}{r}\beta_r = 0, \quad (7)$$

$$\beta + \alpha_{rr} - \frac{1}{r}\alpha_r + Er^4 + Fr^2 + G = 0. \quad (8)$$

These equations are solved for

$$\beta(r) = \beta_0 + \beta_2 r^2, \quad (9)$$

and

$$\begin{aligned} \alpha(r) = \alpha_0 + [\alpha_2 + \frac{1}{4}(\beta_0 + G)]r^2 - \frac{1}{8}(\beta_2 + F)r^4 - \\ - \frac{E}{24}r^6 - \frac{1}{2}(\beta_0 + G)r^2 \ln r. \end{aligned} \quad (10)$$

The solution $u(r, z)$ of the GGSE (2) by means of (4), (9) and (10) is plotted in Fig. 2, for $E = -2$, $G = 0.2$, $F = -4$, $\alpha_0 = 1$, $\alpha_2 = -1$, $\beta_0 = -0.1$, and $\beta_2 = 4.1$. Compared with the generalized Solovév solution of Fig. 1 the equilibrium has an external part of open magnetic surfaces and the closed magnetic surfaces in the inner part have less elongation. The generalized Solovév solution (3) is obtained from (4) by choosing $\beta_0 = -G$, $\beta_2 = 2$, $a_0 = -(F + 2E/3 + 2)/8$ and $a_2 = (F + E/2 + 2)/4$.

Returning to Eq. (5), setting $x = z/r$ and assuming $\alpha = \alpha(r, z)$ and $\beta = \beta(r)$ we obtain

$$\begin{aligned} \beta(1 + x^2)w'' &+ (3\beta - 2r\beta_r)xw' + (r^2\beta_{rr} - r\beta_r)w + \\ &+ r^2(\alpha_{rr} + \alpha_{zz} - \frac{1}{r}\alpha_r + Er^4 + Fr^2 + G) = 0. \end{aligned} \quad (11)$$

This equation is satisfied by $\beta(r) = r^\nu$ and by any solution of the following equations

$$(1 + x^2)w''(x) + (3 - 2\nu)xw'(x) + \nu(\nu - 2)w(x) = 0, \quad (12)$$

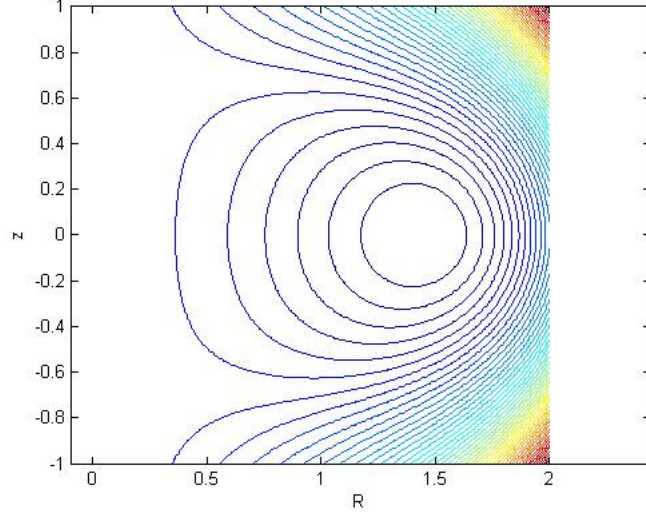


Figure 2: The equilibrium configuration determined by (4) in conjunction with (9) and (10).

$$\alpha_{rr} + \alpha_{zz} - \frac{1}{r}\alpha_r + Er^4 + Fr^2 + G = 0. \quad (13)$$

Equations (12) and (13) constitute a new similarity reduction of the GGSE. Here we note an error in Eq. (15) of [1] which is *not* a solution of Eq. (13) of [1] neither for $\nu = 1/2$ nor for $\nu = 3/2$.

For $\nu = 1$ we obtain the solution of Eq. (12) in the following two equivalent forms

$$\begin{aligned} w &= c_1[x + \sqrt{x^2 + 1}] + c_2[x + \sqrt{x^2 + 1}]^{-1}, \\ w &= d_1\sqrt{x^2 + 1} + d_2x, \end{aligned} \quad (14)$$

where c_1, c_2, d_1, d_2 are arbitrary integration constants. The solution for $\nu = 1$ is given by

$$u(r, z) = \alpha(r, z) + r[c_1[x + \sqrt{x^2 + 1}] + c_2[x + \sqrt{x^2 + 1}]^{-1}], \quad (15)$$

where $\alpha(r, z)$ is any solution of the GGSE such as the generalized Solovév solution and $x = z/r$. It is plotted in Fig. 3, for $E = -2$, $G = 0.2$, $F = -4$, $c_1 = c_2 = 0.05$. The bounding flux surface corresponds to $U_b = 0.40$. Although the configuration is similar to that of Fig. 1, it does not have X-points.

For $\nu = 1/2$ and $\nu = 3/2$ Eq. (12) can't be solved analytically and it has been solved numerically. The solutions are plotted in Figs. 4, 5, 6 and 7. Specifically, for $\nu = 1/2$ we integrated numerically Eq. (12) in the interval $-5 \leq x \leq 5$ for $w(-5) = -1$ and $w'(-5) = 1$. Numerical fitting with a polynomial of ninth order gives

$$\begin{aligned} w(x) &= 0.0002x^9 - 0.0008x^8 - 0.0151x^7 + 0.0481x^6 + 0.3697x^5 \\ &\quad - 1.0552x^4 - 4.4810x^3 + 12.2627x^2 + 55.5659x + 55.8746. \end{aligned}$$

This is plotted in Fig. 4. The respective solution of Eq. (4) for $E = -2$, $G = 0.2$, $F = -4$, is plotted in Fig. 5, where $u = u_{Sol} + cr^{1/2}w$ with u_{Sol} being the generalized

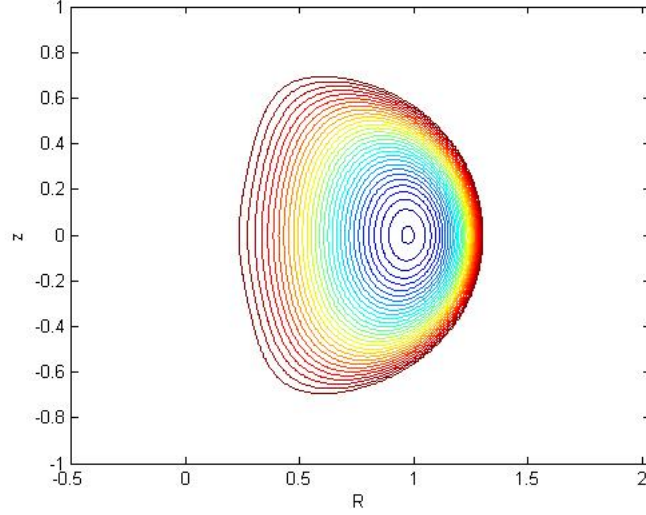


Figure 3: The up-down symmetric equilibrium configuration with smooth bounding surface in connection to the solution (15) of the GGSE (2).

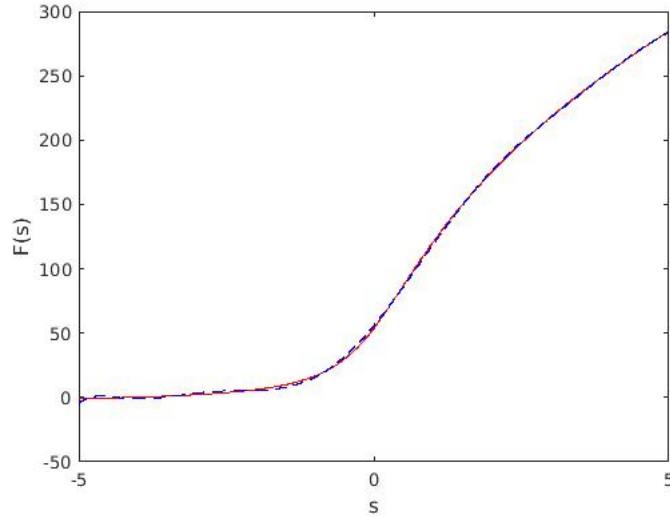


Figure 4: The numerical solution of Eq. (12) for $\nu = 1/2$ (red solid line) versus the polynomial fit (dashed blue line).

Solovév solution (3) and $c = 5 \times 10^{-4}$. The same procedure applies for the case $\nu = 3/2$. We integrated numerically Eq. (12) in the interval $-5 \leq x \leq 5$ for $w(-5) = -1$ and $w'(-5) = 1$. Numerical fitting with a quintic polynomial gives

$$w(x) = -0.0037x^5 - 0.0178x^4 + 0.2269x^3 + 1.8353x^2 + 5.2115x + 6.8747.$$

This is plotted in Fig. 6. The solution of Eq. (4) for $E = -2$, $G = 0.2$, $F = -4$, is plotted in Fig. 7, where $u = u_{Sol} + cr^{3/2}w$ with $c = 5 \times 10^{-3}$. It is noted that the equilibrium configurations in Figs. 5 and 7 are up-down asymmetric.

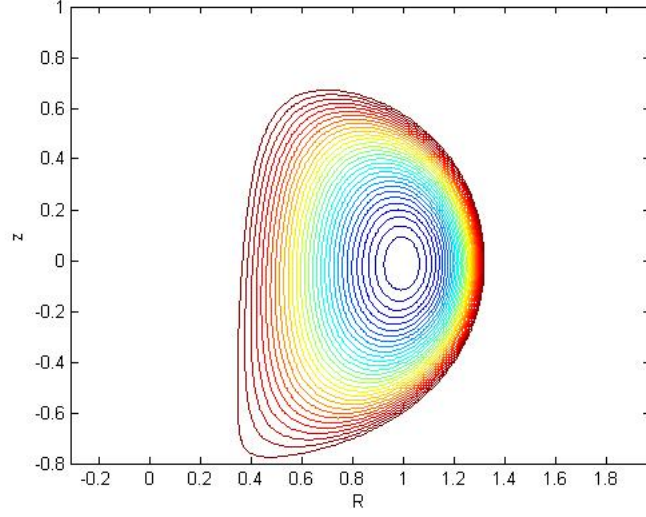


Figure 5: Up-down assymetric equilibrium determined by (4) with the aid of the numerical solution of Eq. (12) for $w(x)$ with $\nu = 1/2$, shown in Fig. 4.

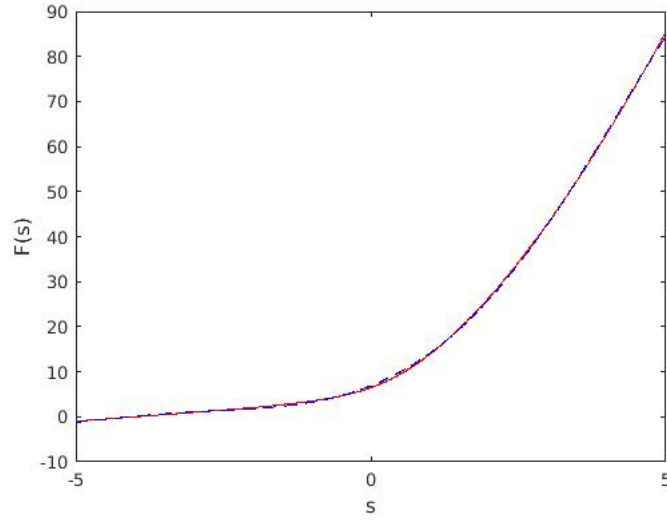


Figure 6: The numerical solution of Eq. (12) for $\nu = 3/2$ (red solid line) versus the polynomial fit (dashed blue line).

For $\nu = 3$ we obtain the explicit solution of Eq. (12) as

$$w = c_1[(x^2 - 2)\sqrt{x^2 + 1} + 3x \sinh^{-1}(x)] + c_2x. \quad (16)$$

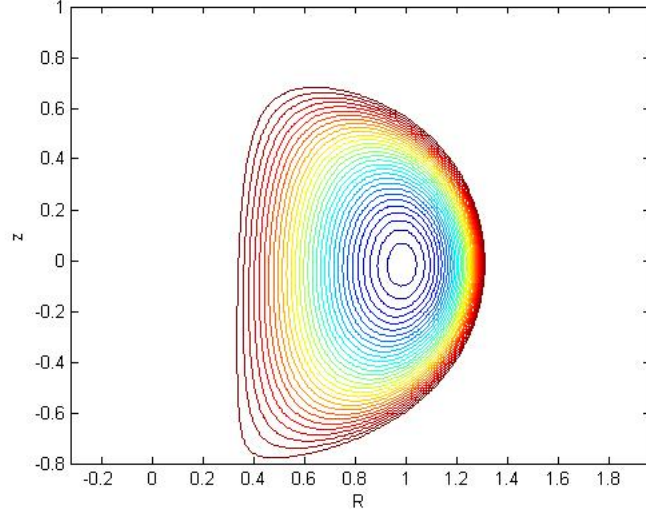


Figure 7: Up-down assymetric equilibrium determined by (4) with the aid of the numerical solution of Eq. (12) for $w(x)$ with $\nu = 3/2$, shown in Fig. 6.

3 More equilibria from similarity reduction

For a general ν Eq. (12) has precisely the general solution [1]

$$\begin{aligned} w(x) = & c_1(1+x^2)^{\frac{(2\nu-1)}{4}} P_{1/2}^{\frac{(1-2\nu)}{2}}(ix) + \\ & + c_2(1+x^2)^{\frac{(2\nu-1)}{4}} Q_{1/2}^{\frac{(1-2\nu)}{2}}(ix), \end{aligned} \quad (17)$$

in terms of the associated Legendre functions $P_{1/2}^{(1-2\nu)/2}(ix)$ and $Q_{1/2}^{(1-2\nu)/2}(ix)$. New non-trivial solutions to the GGSE can be generated from any solution to Eq. (13). For example, we will employ the following solutions to Eq. (13):

$$\alpha(r, z) = -\frac{E}{24}r^6 - \frac{1}{8}Fr^4 - \frac{1}{2}Gz^2, \quad (18)$$

$$\alpha(r, z) = -\frac{E}{24}r^6 - \frac{1}{8}Fr^4 + \frac{G}{2}r^2 \ln r - Gz^2. \quad (19)$$

Using Eq. (17) for $\nu = 3$ and (18) we have the solution

$$\begin{aligned} u(r, z) = & c_1[(z^2 - 2r^2)\sqrt{r^2 + z^2} + 3r^2z \sinh^{-1}\left(\frac{z}{r}\right)] + \\ & + c_2r^2z - \frac{E}{24}r^6 - \frac{1}{8}Fr^4 - \frac{1}{2}Gz^2. \end{aligned} \quad (20)$$

Yet another way to produce new solutions is to consider $\alpha = \alpha(r)$ in Eq. (13) leading to the solution

$$\alpha(r) = d_1r^2 + d_2 - \frac{E}{24}r^6 - \frac{F}{8}r^4 - \frac{1}{2}Gr^2 \ln r. \quad (21)$$

In this case using again the solution (17) for $\nu = 3$ we find from (4)

$$u(r, z) = c_1[(z^2 - 2r^2)\sqrt{r^2 + z^2} + 3r^2 z \sinh^{-1}\left(\frac{z}{r}\right)] + c_2 r^2 z + \alpha_1(r). \quad (22)$$

Moreover if $u(r, z)$ is a solution to the GGSE (2) then $u(r, z) + \beta(r, z)w[x(r, z)]$ is also a solution, thus making it possible to combine solutions with different ν . As an example, combining the solutions for $\nu = 3$ with those for $\nu = 1$ presented previously and Eq. (18) we find

$$\begin{aligned} u(r, z) = & c_1 \left[(z^2 - 2r^2)\sqrt{r^2 + z^2} + 3r^2 z \sinh^{-1}\left(\frac{z}{r}\right) \right] + \\ & + c_2 r^2 z - \frac{E}{24} r^6 - \frac{F}{8} r^4 - \frac{1}{2} G z^2 \\ & + c_3 [z + \sqrt{r^2 + z^2}] + c_4 \frac{r^2}{z + \sqrt{r^2 + z^2}}. \end{aligned} \quad (23)$$

This is plotted in Fig. 8, for $E = -2$, $G = -2.2$, $F = -4$, $c_1 = 0.4$, $c_2 = c_3 = c_4 = 0$. The bounding flux surface corresponds to $U_b = -0.05$ while at the center we have $U_c = -0.2$. Note that this equilibrium configuration has inverse D-shape. Such equilibria

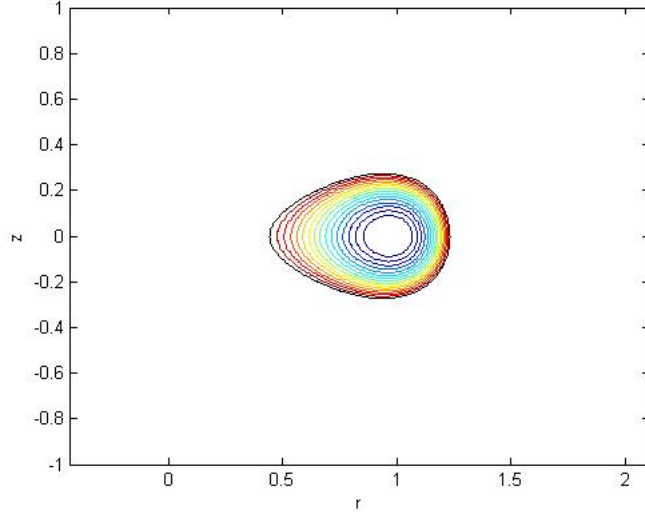


Figure 8: Equilibrium with negative triangularity associated with the solution (23).

has been the subject of recent tokamak studies because they may exhibit improved confinement properties [23, 24].

The family of solutions above contains the classical and non-classical group-invariant solutions of the GGSE so that it greatly extends the range of available analytical solutions. It is interesting that all group-invariant solutions to the GGSE are in fact particular cases of the above similarity reduction. Indeed, Eq. (12) with $\nu = 0$ is solved for

$$w(x) = \frac{c_1 x}{\sqrt{1 + x^2}} + c_2. \quad (24)$$

Adding a particular solution by Eq. (21) we are led to

$$u_3(r, z) = c_1 \frac{z}{\sqrt{r^2 + z^2}} + c_2 + \frac{1}{2} G r^2 (1 - \ln r) - \frac{1}{8} F r^4 - \frac{E}{24} r^6. \quad (25)$$

This is the $U_{inv}^{(3)}(x, y)$ -solution of [3] given by Eq. (23) therein. For $\nu = 1$ a solution of (12) is the second of (14):

$$w(x) = c_1 \sqrt{1+x^2} + c_2 x, \quad (26)$$

while for $\nu = -1$ we solve Eq. (12) for

$$w(x) = \frac{c_1}{(1+x^2)^{3/2}} + c_2 \left[\frac{x}{1+x^2} + \frac{\sinh^{-1}(x)}{(1+x^2)^{3/2}} \right]. \quad (27)$$

Taking a particular linear combination of (26) and (27) and $a(r)$ from Eq. (21) leads to

$$\begin{aligned} u_1(r, z) &= c_1 \sqrt{r^2 + z^2} + c_2 \frac{r^2}{(r^2 + z^2)^{3/2}} + \\ &+ \frac{1}{3} G r^2 - \frac{E}{24} r^6 - \frac{F}{8} r^4 - \frac{1}{2} G r^2 \ln r. \end{aligned} \quad (28)$$

This is the $U_{inv}^{(1)}(x, y)$ -solution of [3] given by Eq. (21) therein. Finally, Eq. (12) with $\nu = 2$ is solved for

$$w(x) = c_1 x \sqrt{1+x^2} + c_2 \sinh^{-1}(x) + c_3. \quad (29)$$

Using $\alpha(r, z)$ from Eq. (19) we have

$$\begin{aligned} u_2(r, z) &= c_1 z \sqrt{r^2 + z^2} + c_2 r^2 \sinh^{-1} \left(\frac{z}{r} \right) + c_3 r^2 - \\ &- G z^2 - \frac{E}{24} r^6 - \frac{F}{8} r^4 + \frac{G}{2} \ln r, \end{aligned} \quad (30)$$

which is the $U_{inv}^{(2)}(x, y)$ -solution of [3] given by Eq. (22) therein.

4 Equilibria from a new similarity reduction

We consider now a new similarity reduction not considered in [1]. Returning to Eq. (12) and setting $x = (r^2 + z^2)/r$, $\alpha = \alpha(r, z)$, $\beta = \beta(r)$ with $2\beta_r - (1/r)\beta = 0$, implying that $\beta = \beta_0 r^{1/2}$, we obtain

$$x^2 w'' + 2xw' - \frac{3}{4}w = 0, \quad (31)$$

$$\alpha_{rr} + \alpha_{zz} - \frac{1}{r}\alpha_r + E r^4 + F r^2 + G = 0, \quad (32)$$

the latter equation being identical with (13). Eq. (31) is solved for

$$w(x) = c_1 \sqrt{x} + \frac{c_2}{x^{3/2}}. \quad (33)$$

Using the solution (19) of Eq. (13) for $\alpha(r)$ we find the solution

$$\begin{aligned} u(r, z) &= -\frac{E}{24} r^6 - \frac{F}{8} r^4 + \frac{G}{2} r^2 \ln r - G z^2 + \\ &+ r^{1/2} \left[c_1 \left(\frac{r^2 + z^2}{r} \right)^{1/2} + c_2 \left(\frac{r^2 + z^2}{r} \right)^{-3/2} \right]. \end{aligned} \quad (34)$$

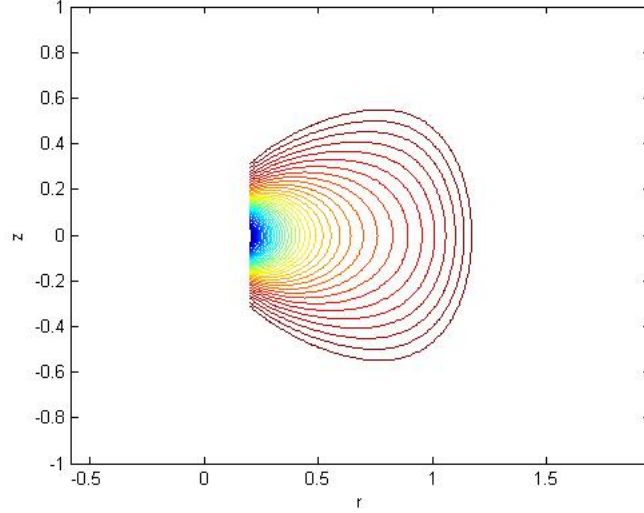


Figure 9: Equilibrium configuration in connection with the solution (34) pertinent to part of a planetary magnetosphere.

This is plotted in Fig. 9, for $E = -2$, $G = -1.2$, $F = -4$, $c_1 = c_2 = -1$. Such a solution could be useful in modelling parts of planetary magnetospheres, e.g., the earth’s magnetosphere, for distances not far from the planet surface [25, 19, 22] and also emerging flux ropes in the solar corona.

5 Conclusions

We have considered a similarity reduction of the GGSE along the lines presented in [1]. New classes of exact solutions to the GGSE were produced, with the generalized Solovév solution being a particular case, describing a variety of D-shaped equilibrium configurations exhibiting up-down symmetry or asymmetry and either positive or negative triangularity. All group-invariant solutions of the GGSE presented in [3] are shown to be particular cases of the above formalism. In addition, a new class of solutions, not considered in [1], has been constructed which can describe part of a planetary magnetosphere for short distances from the planet surface.

Acknowledgments

This work has received funding from the National Fusion Programme of the Hellenic Republic—General Secretariat for Research and Innovation.

References

- [1] Y. E. Litvinenko, Phys. Plasmas **17**, 074502 (2010).
- [2] R. L. White and R. D. Hazeltine, Phys. Plasmas **16**, 123101 (2009).
- [3] A. Kuiroukidis and G. N. Throumoulopoulos, Phys. Plasmas **23**, 112508 (2016).

- [4] L. S. Solovév, Sov. Phys. JETP **26**, 400 (1968).
- [5] F. Hernegger, in Proceedings of the 5th Conference on Controlled Fusion, Vol. I Commissariat a l' Energie Atomique (Grenoble, 1972), p. 26; E. K. Maschke, Plasma Phys. **15**, 535 (1973)
- [6] A. I. Morozov and L. S. Solovév, Rev. Plasma Phys. **8**, 1 (1980).
- [7] H. Tasso and G. N. Throumoulopoulos, Phys. Plasmas **5**, 2378 (1998).
- [8] Ch. Simintzis, G. N. Throumoulopoulos, G. Pantis and H. Tasso, Phys. Plasmas **8**, 2641 (2001).
- [9] D. A. Kaltsas and G. N. Throumoulopoulos, Phys. Plasmas **21**, 084502 (2014).
- [10] C. V. Atanasiu, S. Gunter, K. Lackner and I. G. Miron, Phys. Plasmas **11**, 3510 (2004).
- [11] D. A. Kaltsas, A. Kuiroukidis, and G. N. Throumoulopoulos, Phys. Plasmas **26** 124501 (2019).
- [12] G. Cicogna, F. Ceccherini and F. Pegoraro, J. Phys. A: Math. Gen. **38**, 4597 (2005).
- [13] G. Cicogna, F. Ceccherini and F. Pegoraro, *Integrability and Geometry: Methods and Applications* (SIGMA, 2006), Vol. 2, p. 017.
- [14] A. Kuiroukidis and G. N. Throumoulopoulos, Phys. Plasmas **22** 084502 (2015).
- [15] P. Olver, *Applications of Lie Groups to Differential Equations* (Springer-Verlag, New York, 1993).
- [16] E. Tassi, F. Pegoraro and G. Cicogna, Phys. Plasmas **15**, 092113 (2008).
- [17] P. J. Mc Carthy, Phys. Plasmas **6**, 3554 (1999).
- [18] A. J. Cerfon and J. P. Freidberg, Phys. Plasmas **17**, 032502 (2010).
- [19] G. Poulipoulis and G. N. Throumoulopoulos, Phys. Plasmas **30**, 114501 (2023).
- [20] M. Frewer, M. Oberlack and S. Guenther, Fluid Dyn. Res. **39**, 647 (2007).
- [21] D. A. Kaltsas and G. N. Throumoulopoulos, Phys. Lett. A **380**, 3373 (2016).
- [22] A. Lukin, I. Vasko, A. Artemyev, and E. Yushkov, Phys. Plasmas **25**, 012906 (2018).
- [23] M. E. Austin, A. Marinoni, M. L. Walker, M.W. Brookman, J. S. deGrassie, A.W. Hyatt et al., Phys. Rev. Lett. **122**, 115001 (2019).
- [24] G. Merlo, Z. Huang, C. Marini, S. Brunner, S. Coda, D. Hatch et al., Plasma Phys. Control. Fusion **63**, 044001 (2021).
- [25] J. E. Borovsky and J. A. Valdivia, Surv. Geophys. **39**, 817 (2018).